Computational study of the cavitation phenomenon and its interaction with the turbulence developed in diesel injector nozzles by Large Eddy Simulation (LES)

F.J. Salvador[a,*], J. Martínez-López[a], J.-V. Romero[b], M.-D. Roselló[b]

[a]*CMT- Motores Térmicos, Universitat Politècnica de València, Camino de Vera s/n, Edificio 6D, 46022, Valencia, Spain*
[b]*Instituto de Matemática Multidisciplinar, Universitat Politècnica de València, Camino de Vera s/n, Edificio 8G, 2º, 46022, Valencia, Spain*

Abstract

In the present paper, a homogeneous equilibrium model with a barotropic equation of state has been used for modeling cavitation in a real multi-hole microsac nozzle. The turbulence effects have been taking into account by Large Eddy Simulation (LES), using the Smagorinsky model as the sub-grid scale turbulent model and the Van Driest model for the wall damping.

Firstly, the code has been validated at real operating diesel engine conditions with experimental data in terms of mass flow, momentum flux and effective velocity, showing that the model is able to predict with a high level of confidence the behavior of the internal flow at cavitating conditions. Once validated, the code has allowed to study in depth the turbulence developed in the discharge orifices and its interaction with cavitation phenomenon.

Keywords: cavitation, Large Eddy Simulation, internal flow, diesel injector

1. Introduction

Most of the improvements achieved to reduce the emissions of diesel engines and improve their efficiency are due thanks to the advances in fuel injection systems. One of the most widely used strategies in recent years has been the increase of injection pressure, which has forced that cavitation and turbulence play a fundamental role on the internal flow and spray development [1, 2].

The experimental study of the turbulence developed within diesel injector nozzles and its interaction with cavitation phenomenon present huge difficulties due to extremely small size of the holes, the existence of a multiphase flow and the high velocities found in the discharge orifices, so the use of Large Eddy Simulation (LES) has become a great alternative to advance in the knowledge of the internal flow [3, 4]. This technique, which captures the large scale motions of the flow and models the small scale motions that occur on length scales smaller than the mesh spacing, can be viewed as a bridge between Direct Numerical Simulation (DNS) and the cheapest method to model turbulent flows, Reynolds Averaged Navier-Stokes (RANS).

In the present paper, a homogeneous equilibrium model has been used for modeling cavitation in a diesel injector nozzle simulating real operating engine conditions. The paper has been organized in the following way. Firstly, a complete description of the code used to model cavitation will be presented in section 2. Secondly, the details of the multihole nozzle and the general setup of the simulations will be presented in section 3. The results obtained in the validation of the code, comparing numerical results against experimental ones in terms of mass flow, momentum flux and effective velocity will be shown in section 4. The vapour phase distribution and its interaction with the turbulence developed within the nozzle will be raised in sections 5 and 6 respectively. Finally, the main conclusions of the study will be drawn in section 7.

---

*Corresponding author: Dr. F. Javier Salvador, Tel.: +34 9638779659; fax: +34 963877659.
Email addresses: `fsalvado@mot.upv.es` (F.J. Salvador), `jormarlo@mot.upv.es` (J. Martínez-López), `jvromero@imm.upv.es` (J.-V. Romero), `drosello@imm.upv.es` (M.-D. Roselló)

2. Cavitation modelling

Due to high velocities and pressures that occur in diesel injectors nozzles, the use of a homogeneous equilibrium model (HEM), which assumes that liquid and vapour phases are always perfectly mixed, together with a barotropic equation of state seems to be the most suitable method to model cavitation phenomenon [5].

This barotropic equation (Eq. (1)) relates pressure and density through the compressibility of the mixture, which is the inverse of the speed of sound squared (Eq. (2)):

$$\frac{D\rho}{Dt} = \Psi \frac{Dp}{Dt}, \tag{1}$$

$$\Psi = \frac{1}{a^2}. \tag{2}$$

Eq. (1) can be introduced directly in the continuity equation to formulate a pressure equation, and must be consistent with the liquid and vapour equations of state both at the limits when there is pure liquid or pure vapour, and also at intermediate states when there is a mixture of both phases.

At these limits, the density of the liquid and vapour phases can be defined with a linear equation of state:

$$\rho_v = \Psi_v \cdot p, \tag{3}$$

$$\rho_l = \rho_l^0 + \Psi_l \cdot p, \tag{4}$$

where ρ_l^0 is liquid density at a given temperature condition.

The amount of vapour in the fluid is determined with the γ parameter (Eq. (5)), which is 0 in a flow without cavitation and 1 for fully cavitated flows,

$$\gamma = \frac{\rho - \rho_{l\,sat}}{\rho_{v\,sat} - \rho_{l\,sat}}, \tag{5}$$

where

$$\rho_{v\,sat} = \Psi_v \cdot p_{sat}. \tag{6}$$

The density of the mixture is calculated taking into account the amount of vapour in the fluid (γ) together with a correction term based on the pressure (mixture's equilibrium equation of state):

$$\rho = \gamma \cdot \rho_v + (1 - \gamma) \cdot \rho_l + \Psi \cdot (p - p_{sat}). \tag{7}$$

With regard to the mixture's compressibility and viscosity, they are modeled by a simple linear model as a function of the amount of vapour in the fluid:

$$\Psi = \gamma \cdot \Psi_v + (1 - \gamma) \cdot \Psi_l, \tag{8}$$

$$\mu = \gamma \cdot \mu_v + (1 - \gamma) \cdot \mu_l. \tag{9}$$

As far as the methodology used by the solver is concerned, the code starts solving the continuity equation for the density (Eq. (10)):

$$\frac{\partial \rho}{\partial t} + \nabla \cdot (\rho \vec{u}) = 0. \tag{10}$$

The value of density obtained, is used to determine preliminary values of gamma and compressibility by means of Eq. (5) and Eq. (8), and also, for solving momentum equation (Eq. (11)) which is used to get the matrices used to calculate the pressure-free velocity, $\vec{u}$:

$$\frac{\partial (\rho \vec{u})}{\partial t} + \nabla \cdot \left(\rho \frac{\vec{u}\vec{u}}{2} \right) = -\nabla p + \nabla \cdot (\mu \nabla \vec{u}) - \nabla \tau. \tag{11}$$

The last term of this equation ($\nabla \tau$) represents the Sub-Grid Scale-Stress used in Large Eddy Simulation, and it has been estimated with the Smagorinsky model (which is one of the most appropriate methods to model channels and internal flow [3, 4, 6]), taking into account the influence of the wall in the turbulence dynamic with the Van Driest damping model.

Following, an iterative PISO algorithm is used to solve for p and correct the velocity to achieve continuity. The equation solved for the PISO loop is the continuity equation transformed into a pressure equation by use of the equation of state (Eq. (7)):

$$\frac{\partial(\Psi p)}{\partial t} - \left(\rho_1^0 + (\Psi_1 - \Psi_v)p_{\text{sat}}\right)\frac{\partial \gamma}{\partial t} - p_{\text{sat}}\frac{\partial \Psi}{\partial t} + \nabla \cdot (\rho \vec{u}) = 0. \tag{12}$$

Once continuity has been reached, the amount of vapour, density and compressibility are updated by means of Eqs. (5), (7) and (8) respectively, which are taken into account to solve again momentum equation, and therefore, repeating the algorithm until convergence.

3. Nozzle simulated and simulation setup

The nozzle studied in the present paper is a cilindrical six-hole microsac nozzle (and so, it is inclined to cavitate [7, 8]) with a diameter of 170 μm, 1 mm of length and a curvature inlet radius of 13 μm.

The domain simulated belongs to only one orifice of the whole nozzle in order to reduce the high computational cost typical of Large Eddy Simulation techniques. The geometry, which simulates fully needle lift conditions, includes all the volume occupied by the fuel between the needle and the nozzle internal wall, the needle seat and the orifice, where the fuel flows toward the combustion chamber of the engine (see Fig. 1). The domain has been discretized in a hybrid mesh of 1.836.964 cells, with cell size ranging in the orifice from 0.6 μm in the orifice wall to 3 μm in the orifice core (D/56.7) and 8 μm in the rest of the geometry (sac and the zone between the needle and the nozzle wall).
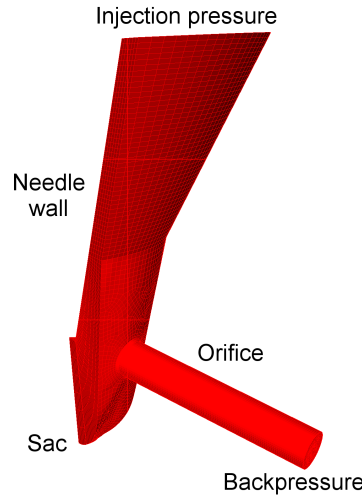

Figure 1: Multi-hole nozzle simulated.

As far as the main boundary conditions are concerned, a fixed pressure condition has been used for the definition of the injection pressure. Despite of some authors advice to use precursor simulation methods [9], not only no differences were found in the numerical results obtained in different simulation tests, but also the use of these boundary conditions greatly increased the computational cost. On the other hand, a mean pressure boundary condition has been applied at the outlet section to simulate the pressure of the combustion chamber. This boundary keeps the mean value desired, allowing zones with very low pressures due to the presence of vapour bubbles, avoiding the imposition of a rigorous boundary condition at the orifice outlet that could affect the nature of the vapour structures formed within the nozzle. With regard to the velocity, a non-slip condition has been applied at the orifice walls.

For validation purpose and subsequent study of the cavitation and turbulence interaction, four simulations have been calculated fixing the injection pressure to 160 MPa and varying the backpressure to 3, 5, 7 and 9 MPa. Each simulation has been run in parallel using 30 processes, needing 90 days to complete 100 μs.

3

4. Validation of the code

Before studying in depth the cavitation and turbulence developed in the nozzle, it is necessary to check the potential of the code for modeling the internal flow in diesel injector nozzles at cavitating conditions. This validation has been performed in terms of mass flow, momentum flux and effective velocity, comparing the results provided by the code against experimental data.

The experimental results of mass flow and momentum flux have been obtained with an Injection Rate Discharge Curve Indicator (IRDCI) commercial system and a Momentum flux test rig [1] respectively. The injection rate meter, based on Bosch method [10] provides a mass flow measurement with an uncertainty value of 1.5%, whereas the Momentum flux test rig, which determines the impact force of a spray with a piezo-electric pressure sensor, allows to measure with an uncertainty of around 1.8%. Combining both measurements, it is possible to determine another useful parameter in the hydraulic characterization of a nozzle, the effective velocity at the outlet section.

Fig. 2 shows the comparison of both results for the mass flow (left), momentum flux (center) and effective velocity (right). For all the pressure condition simulated, the mean value has been represented as a function of the root of pressure drop, being the pressure drop the difference between the injection pressure (160 MPa) and the backpressure (3, 5, 7 and 9 MPa). The time averaged corresponds to a period equal to 15 times the time needed by a fluid particle to cover the whole orifice.
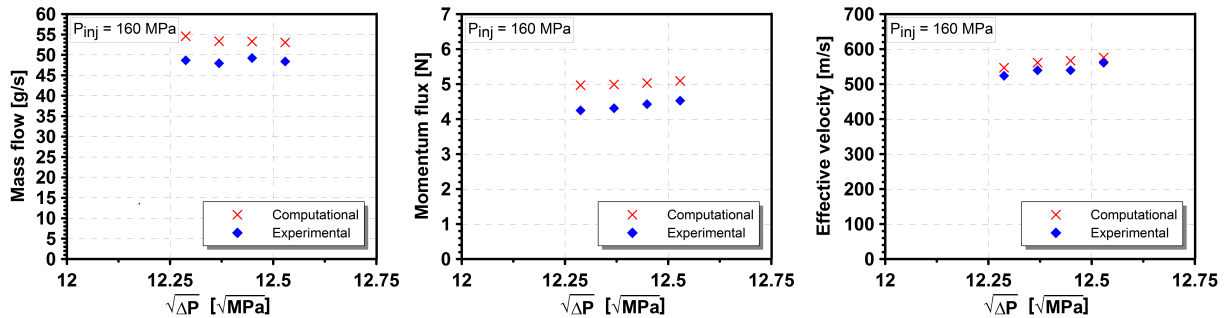

Figure 2: Comparison of experimental and numerical results.

As can be observed, for all the parameters and pressure conditions compared, CFD calculations slightly overestimate the experimental results, following always the tendencies of the experimental data.

Attending to the mass flow injected by the nozzle, represented in the left plot, it can be seen that the mass flow is collapsed in both cases, keeping constant for all the pressure conditions. This indicates that the flow is at cavitating conditions [11, 12]. The deviation between experimental and computational values is around 10%. However, due to the measurements uncertainties in the determination of the mass flow, momentum flux, and the internal geometry by the silicone technique [13], and the complexity of modeling cavitating flows it can be considered that the code is able to predict the behavior of the flow with enough degree of confidence.

Opposite to the mass flow behavior, the momentum flux represented in the plot placed in the middle of Fig. 2 is not choked, so an increment of effective velocity is expected since it is calculated dividing the momentum flux values by the mass flow. Effectively, as can be seen on the right of Fig. 2, the effective velocity experiments a linear increase with the square root of pressure drop, reaching values of almost 600 m/s, with a deviation between experimental and computational results for the velocity always lower than 5%. This velocity rise is justified by the fact that the presence of vapour near the orifice wall due to cavitation phenomenon reduces the friction losses (slip condition) and the effective diameter for the liquid phase [1].

5. Vapour phase distribution

Attending to the mass flow results seen in Fig. 2, it is expected to see vapour bubbles into the discharge orifices for any pressure condition simulated, since the mass flow remains collapsed due to cavitation phenomenon.

4

In order to asses it, Fig. 3 shows the vapour field averaged (where blue regions correspond to pure liquid and red regions correspond to pure vapour) at seven cross section of the orifice and its standard deviation for the simulation $P_{inj} = 160$ MPa $- P_{back} = 5$ MPa, averaging the same time used for the mass flow, momentum flux and velocity results.

As expected, the average field shows as the vapour bubbles are distributed along the upper part of the orifice, being the origin of the vapour phase the inlet corner region of the channel. The vapour bubbles flow along the upper surface of the orifice wall reaching the exit although it is possible to see vapour phase in the center and lower part of the orifice near the outlet section. Furthermore, the standard deviation values indicate that cavitation is always present near the orifice inlet, whereas cavitation appearance as the bubbles reach the exit varies time step to time step, showing that cavitation is a transient phenomenon.
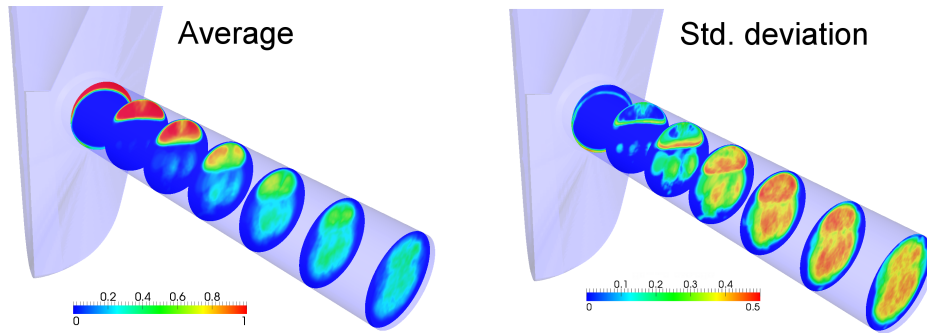

Figure 3: Vapour phase average and standard deviation.

The existence of vapour bubbles in the nozzle, similar to seen in the rest of backpressures simulated, confirms the results previously obtained in section 4, where cavitation was detected when the mass flow remained constant in spite of decreasing the backpressure.

6. Turbulence and vapour phase interaction

The reduced dimensions of a diesel nozzle, together with the high velocities found inside the discharge orifices for real operating conditions of diesel engines ensure a turbulent flow regime. As a sample of the flow regime at pressure conditions simulated in the present paper, for the case $P_{inj} = 160$ MPa $- P_{back} = 5$ MPa, Reynolds number is around 9500.

Fig. 4 shows the streamlines colored by velocity, from the inlet boundary condition where injection pressure is adjusted, to the outlet section of the orifice. The streamlines, which show the direction of a fluid particle at any point in time, allow to observe the formation of eddies in the nozzle sac just before the hole. The zoomed picture makes easier the visualization of these vortices developed, which has a strong influence on the cavitation distribution, especially near the inlet orifice.

The influence of the turbulence on the cavitation appearance can be seen in Fig. 5, where vapour phase has been depicted for several cross sections of the orifice. Vapour phase is clearly divided in two cores, which can be also observed representing the velocity vectors in one of the cross sections chosen of the orifice. The direction of the vectors shows a pair of twin vortices, one of them in the left part, and another one in the right part of the section. This behavior, which has been observed by other authors [14], justifies the separation of the vapour phase in two regions.

Up to now, it has been proved that the turbulence developed inside a diesel injector nozzle has a strong influence on the vapour phase appearance. Nevertheless, there is a certain interaction or interdependence between both phenomena, since cavitation also enhances turbulence [7, 15]. Indeed, if the vapour phase within the nozzle is compared with the vorticity (see Fig. 6) it is possible to state that the highest values of turbulence is due to the presence of vapour bubbles, reaching the maximum values in the interphase liquid-vapour region.

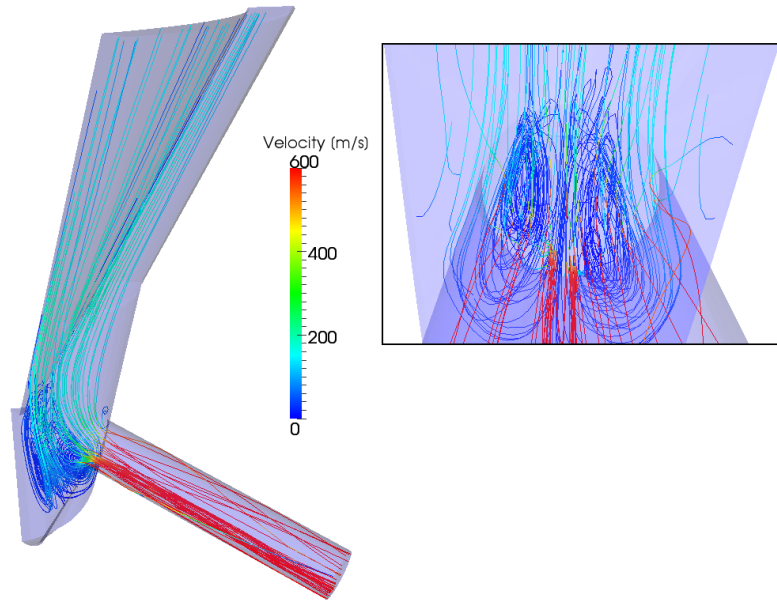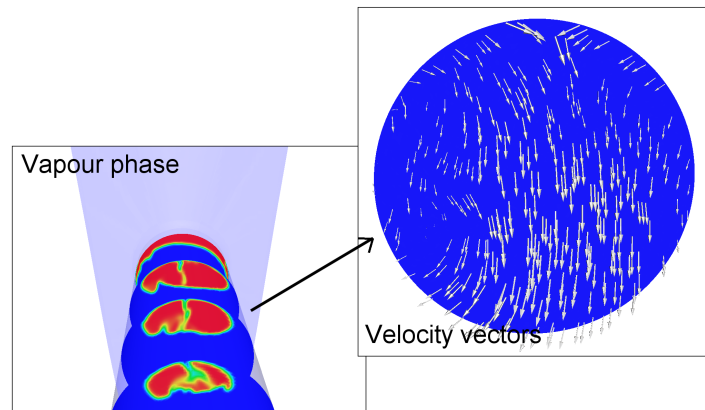Figure 4: Streamlines for the simulation and zoomed area of the sac and orifice inlet. $P_{inj} = 160$ MPa $- P_{back} = 5$ MPa.

Figure 5: Vapour phase and velocity vectors for the simulation $P_{inj} = 160$ MPa $- P_{back} = 5$ MPa.
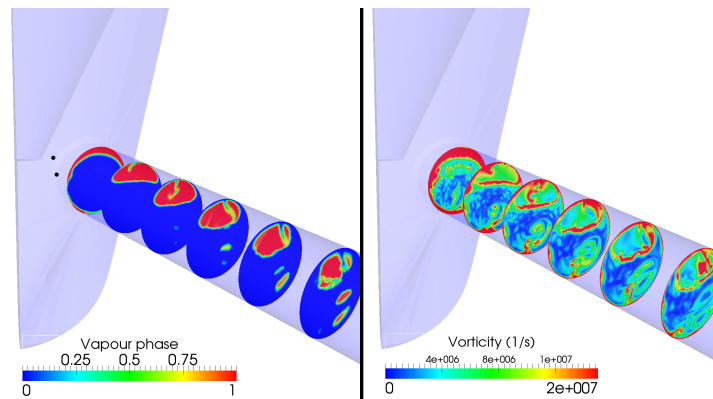
Figure 6: Vapour phase distribution and vorticity ($P_{inj} = 160$ MPa $- P_{back} = 5$ MPa).

7. Conclusions

From the present investigation the following main conclusions can be drawn:

- A code to model cavitation phenomenon has been applied for the simulation of 3D cavitating flows by Large Eddy Simulation.

- An extended validation of the code has been performed in terms of mass flow, momentum flux and effective velocity in a diesel injector nozzle at real operating conditions, showing an acceptable level of confidence.

- Cavitation appearance is strongly influenced by the turbulence and vortices development, justifying the separation of the vapour phase in two cores in the zone near the orifice inlet.

- Cavitation enhances turbulence, since the highest values of vorticity in the nozzle are found at the interphase liquid-vapour.

Acknowledgments

Nomenclature

a: speed of sound
D: diameter
p: pressure
P_{back}: back pressure
P_{inj}: injection pressure
p_{sat}: vaporisation pressure
t: time

170 $\vec{u}$: velocity

Greek symbols:

172 γ: vapour fraction

173 ΔP: pressure drop, $\Delta P = P_{inj} - P_{back}$

174 μ: fluid viscosity

175 ρ: fluid density

176 $\rho_{l\,sat}$: liquid density at saturation

177 ρ_l^0: liquid density at a given temperature condition

178 $\rho_{v\,sat}$: vapour density at saturation

179 τ: Sub-Grid Scale-Stress

180 Ψ: fluid compressibility

Subscripts:

182 l: liquid

183 v: vapour

References

[1] R. Payri, J. M. García, F. J. Salvador, J. Gimeno, Using spray momentum flux measurements to understand the influence of diesel nozzle geometry on spray characteristics, Fuel 84 (2005) 551–561.

[2] H. K. Suh, C. S. Lee, Effect of cavitation in nozzle orifice on the diesel fuel atomization characteristics, International journal of heat and fluid flow 29 (2008) 1001–1009.

[3] U. Piomelly, Large-eddy simulation: achievements and challenges, Progress in Aerospace Sciences 35 (4) (1999) 335–362.

[4] R. Payri, B. Tormos, J. Gimeno, G. Bracho, The potential of Large Eddy Simulation (LES) code for the modeling of flow in diesel injectors, Mathematical and Computer modeling 52 (2010) 1151–1160.

[5] F. P. Kärrholm, Numerical modelling of diesel spray injection, turbulence interaction and combustion, Ph.D. thesis, Chalmers University of Technology (2008).

[6] R. Payri, B. Tormos, J. Gimeno, G. Bracho, Large Eddy Simulation for high pressure flows: Model extension for compressible liquids, Mathematical and Computer modeling 54 (2011) 1725–1731.

[7] F. Payri, V. Bermúdez, R. Payri, F. J. Salvador, The influence of cavitation on the internal flow and the spray characteristics in diesel injection nozzles, Fuel 83 (2004) 419–431.

[8] R. Payri, S. Molina, F. J. Salvador, J. Gimeno, A study of the relation between nozzle geometry, internal flow and spray characteristics in diesel fuel injection systems, KSME International Journal 18 (7) (2004) 1225–1235.

[9] G. R. Tabor, M. H. Baba-Ahmadi, Inlet conditions for large eddy simulation: A review, Computer & Fluids 39 (2010) 553–567.

[10] M. Marcic, Measuring method for diesel multihole injection nozzles, Sensors and actuators 107 (2003) 152–158.

[11] C. Mishra, Y. Y. Peles, Size scale effects on cavitating flows through microorifices entrenched in rectangular microchannels, Journal of microelectromechanical systems 14 (5) (2005) 987–999.

[12] F. J. Salvador, S. Hoyas, R. Novella, J. Martínez-López, Numerical simulation and extended validation of two-phase compressible flow in diesel injector nozzle, Proceedings of the Institution of Mechanical Engineers, Part D, Journal of Automobile Engineering 225 (2011) 545–563.

[13] V. Macián, R. Bermúdez, V. Payri, J. Gimeno, New technique for the determination of the internal geometry of diesel nozzle with the use of the silicone methodology, Experimental techniques 27 (2) (2003) 39–43.

[14] R. Masuda, T. Fuyuto, M. Nagaoka, Validation of a diesel fuel spray and mixture formation from nozzle internal flow calculation, SAE paper 2005–01–2098.

[15] J. M. Desantes, R. Payri, F. J. Salvador, J. De la Morena, Influence of cavitation phenomenon on primary break-up and spray behavior at stationary conditions, Fuel 89 (2010) 3033–3041.